

# Energy-Aware Cooperative Spectrum Sensing under Ignorance on Internet of Mobile Things

KAREL TOLEDO<sup>1</sup> (*Member, IEEE*), JORGE TORRES GÓMEZ<sup>2</sup> (*Senior Member, IEEE*),  
FALKO DRESSLER<sup>2</sup> (*Fellow, IEEE*), AND M. JULIA FERNÁNDEZ-GETINO GARCÍA<sup>3</sup>  
(*Member, IEEE*)

<sup>1</sup>Electrical Engineering Department, Faculty of Engineering, University of Santiago of Chile (USACH), Chile

<sup>2</sup>School of Electrical Engineering and Computer Science, TU Berlin, Berlin, Germany

<sup>3</sup>Department of Signal Theory and Communications, Carlos III University of Madrid, 28911, Leganés, Madrid, Spain

CORRESPONDING AUTHOR: Karel Toledo (e-mail: karel.toledo@usach.cl).

This work was supported in part by the Chilean National Agency for Research and Development ANID Fondecyt Postdoctorado under Grant 3230184, the Federal Ministry of Education and Research (BMBF, Germany) within the 6G Research and Innovation Cluster 6G-RIC under Grant 16KISK020K, and the Spanish National project IRENE-EARTH (PID2020-115323RB-C33 / AEI / 10.13039/501100011033).

**ABSTRACT** The Internet of Things (IoT) enables the interconnection of multiple devices, typically sharing network resources. These devices must identify a suitable time to access the channel without interfering with each other, which can lead to additional energy consumption. To extend the network lifetime, cooperative strategies have been proposed that modify the device operations between the ON/OFF states to conserve energy. However, the challenge of selecting active devices for spectrum sensing increases with mobile agents, referred to as Internet of Mobile Things (IoMT), since their positions may be unknown. To deal with this uncertainty, we propose using the ordered weighted averaging (OWA) operator, which provides a framework for decision-making under ignorance, to model the position uncertainty resulting from node movement. We estimate node positions by assigning representative values for their distances to the fusion center and primary user. We then determine the optimal number of active nodes that minimize energy consumption while meeting detection constraints. We evaluate performance for different scenarios in networks of various sizes consistent with smart agriculture environments, employing optimistic and pessimistic approaches. The quality of decisions is validated under the assumption of nodes governed by particular mobility patterns.

**INDEX TERMS** Cooperative spectrum sensing, decision-making under ignorance, energy efficiency, Internet of Things

## I. INTRODUCTION

THE Internet of Things (IoT) is a network of interconnected devices that collect and exchange data among each other while sharing frequency bands. This paradigm enables novel interactions and communications between the physical and digital realms. The integration of IoT technology has become prevalent across diverse applications, including the agriculture sector [1], [2]. Farmers can improve agricultural efficiency and productivity while minimizing costs and environmental impact by utilizing static and mobile smart devices, such as sensors, unmanned aerial vehicles (UAVs), and robots, in their daily tasks. The spectrum scarcity problem affects these networks as the devices typically operate in overcrowded industrial, scientific,

and medical (ISM) frequency bands. Promoting alternative methods for managing spectrum resources is crucial to avoid interfering with licensed users [3], [4].

Cognitive radio-capable devices can be integrated into IoT networks to address the spectrum scarcity problem. These entities can be classified as secondary user (SU), fusion center (FC), or primary user (PU) based on cognitive radio nomenclature. In this context, devices for smart agriculture or SUs must continuously sense the spectrum to detect available channels for opportunistic transmission of information; PUs are licensed devices for spectrum usage; FC merge the data received from SUs to make a final decision about the availability of spectrum bands.

Each time a SU performs spectrum sensing tasks, it consumes additional energy, which can become critical, primarily when powered by batteries. Therefore, optimal energy usage and management during spectrum sensing are crucial to increasing the lifetime of current IoT networks [5]. To overcome this issue, reported solutions address the problem from two viewpoints mainly: energy harvesting [6], [7] and energy conservation [8], [9]. The first approach involves using the energy harvested by nodes to conduct spectrum sensing operations and recharge batteries [10]. However, external energy sources may be unreliable over time, raising concerns about extending the available energy in sensor nodes. The second approach aims to execute energy-efficient operations from various perspectives, enabling the network to run unattended for as long as possible.

Implementing the ON/OFF policy employed during the cooperative spectrum sensing (CSS) is a widely used strategy to conserve stored energy [11]. These approaches determine the minimum number of active SUs required to successfully detect PU signal and avoid interference with minimal energy consumption. The remaining nodes enter a sleep mode to conserve energy. An optimization problem is usually formulated using an energy metric as the objective function and considering detection constraints for energy minimization. Heuristic algorithms identify the optimal number of active nodes to devise a solution with reduced time complexity.

In general, sensor selection is addressed by assuming the position of devices within the network is known, simplifying the decision-making and enabling strategies under certainty [11]–[16]. However, this precise knowledge is typical of static IoT setups, which do not account for the mobility of nodes within the network, as seen in Internet of Mobile Things (IoMT). At present, IoMT scenarios align with: i) precision agriculture, where UAVs cover a specific area to monitor and assist with fertilizer and herbicide application in crops [17], [18], ii) smart cities, specifically intelligent transportation systems (ITS), where spectrum resource allocation becomes essential to improve communication performance [19], and iii) large-scale events or emergencies, where a flexible mobile network assisted by drone base stations (BSs) provides on-demand connectivity or address temporary increases in network traffic [20]. All previous applications are situated in the context of green communications by prioritizing energy optimization for environmental consciousness.

In order to address the mobility of nodes in such networks, a non-static scenario has been adopted in which the movement of devices adheres to specific rules. This analysis facilitates the computation of two different magnitudes as statistical moments or the probability density function (PDF) of mobility patterns to provide a solution for a given probability [21], [22]. Both approaches, called under risk, are restricted to situations where the decision-maker can derive or estimate the statistical features. From our understanding, a more general approach to conserving energy in real-world networks when ignoring the nodes' position has yet to be

explored. The motivation of this work is to fill the existing gap in determining the appropriate nodes that must be active under ignorance of the mobility pattern.

This paper presents a general strategy to optimize energy consumption during spectrum sensing operations in the IoMT, particularly for decision-making when the positions of nodes are unknown. The unknown positions of SUs are modeled by employing the ordered weighted averaging (OWA) operator [23]. This framework allows mapping the possible values of distances from SUs to the FC and PU into a representative score, ranging from the optimistic case associated with shorter distances to the pessimistic case related to longer distances. Performance evaluation assumes that the decision-maker uses homogeneous and heterogeneous strategies. For different mobility models, the implications of both methodologies in terms of consumed energy and detection reliability are quantified.

Our main contributions can be summarized as follows:

- The IoMT environment is modeled in alignment with smart agriculture, considering the dynamics of SUs. The OWA operator is used for decision-making when the positions of the nodes are unknown, based on the decision-maker's attitude (subjective) and limited knowledge of the node movement patterns (objective).
- A stochastic optimization problem is formulated to reduce the energy consumption in CSS. The feasible solution of a deterministic equivalent version is obtained using OWA-based assumptions regarding the distances of each SU to FC and PU.
- Two approximations are deeply analyzed: one for certain distances representing all nodes, named homogeneous, and the other more general with individual decisions per node, called heterogeneous.
- The energy-aware performance under ignorance is validated through simulations in different network sizes. The impact of decision strategies and the relevance of these results are studied and compared to those reported under risk approaches.

This paper is structured as follows. The related works are exposed in Section II. The system model, channel propagation, and detection theory are presented in Section III. The problem formulation and energy metric related to CSS are discussed in Section IV. Both sensor selection strategies and uncertainty management via OWA operator are proposed in Section V. Section VI provides illustrative examples for scenarios of different network sizes and validates detection constraints. Section VII concludes the paper.

## II. RELATED WORK

The literature outlines five principal methodologies to reduce the energy consumption of nodes and prolong the network lifetime. Energy conservation techniques focus on optimizing the throughput and energy sensing efficiency [24], [25], implementing power allocation techniques for each sensor

[9], optimizing the packet size for transmissions [26], implementing energy-efficient spectrum sensing techniques via machine learning algorithms [27]–[29], and suitable sensor selection with ON/OFF policies [11]–[16].

In the latter approach, sensor selection strategies have been addressed for a scenario with incomplete information about the network status [12] or assuming a multi-channel environment with multiple PUs sharing the spectrum with SUs in the same area [13], [14]. The cluster formation based on spectrum sensing and PU activity is modeled in [15] to derive a relationship between the active nodes and the signal to noise ratio (SNR). The mechanisms to achieve equal energy consumption involve the participation of sensors with a reduced probability of detection in CSS. This approach will help to avoid the rapid depletion of batteries in sensors with higher performance [16].

However, the majority of reported solutions [11]–[16] assume static nodes, which limits their applicability in IoMT environments [30]. This assumption implies that distances from each SU to FC and PU can be considered to be constants. The mobility of nodes introduces a new challenge regarding the evolution of their spatial coordinates over the operational lifetime of the network. This assertion transforms the sensor selection process in dynamic networks into a decision-making problem that can be classified as either under certainty or uncertainty [31].

Certainty scenarios have been modeled as a kind of stochastic programming known as “wait-and-see” [32]. This strategy posits that the positions of nodes remain fixed for a brief period. Thus, the problem is solved by applying the tools of static solutions as discussed above. The proposal in [33] illustrates an example of computing the total number of awake nodes per time slot. However, this method has the drawback of repeating the computation of the optimal solution whenever the sensor nodes change positions, which results in a waste of energy. Moreover, this kind of solution incurs an additional energy cost in reporting the position of SUs to FC.

Uncertainty scenarios can be categorized as either under risk or ignorance. Solutions for scenarios under risk can be addressed using the “here-and-now” approach [34], which involves analyzing the statistical description of movement. A strategy for selecting the optimal active sensors in a dynamic wireless sensor network (WSN) is proposed in [21] through the first and second statistical moments of distances from each SU to FC. A second approach that minimizes random consumed energy is presented in [22] for nodes performing different mobility models, including Random Walk, Random Waypoint, and Gauss-Markov. This method estimates the PDF of random distances from each SU to FC and solves a deterministic equivalent problem to minimize an energy upper bound.

What about decision-making under ignorance? Until now, sensor selection in IoMT has been addressed under certainty or, in cases of uncertainty, under risk. However, decision-

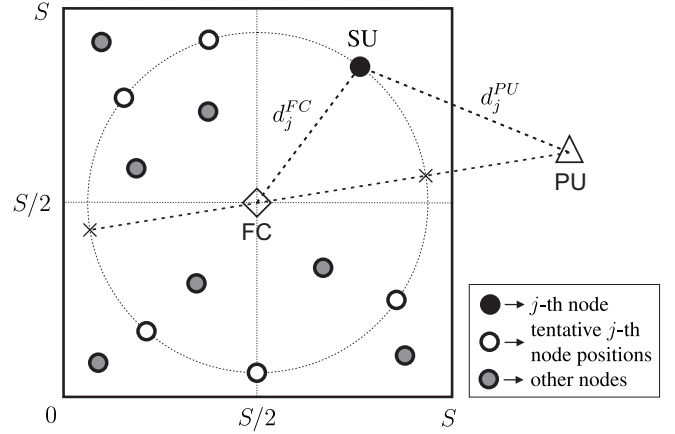


FIGURE 1: System model for an IoMT network.

making can also be implemented under ignorance when the position of each SU is unknown at any given time. The evolution of node positions represents a stochastic process where statistical features such as the PDF and moments are generally assumed to be unknown. Specifically, we have limited environmental knowledge, such as area boundaries, to prevent nodes from moving out of the simulation scenario. To handle this uncertainty, we can use distinct options: a PDF that carries the minimum amount of information [35], replace unknown probabilities with Dempster-Shafer belief functions [36], apply interval calculus to replace probabilities with probability intervals [37], or use the OWA operator to transform a range of performance values into a single representative value [23]. Among these alternatives, the OWA operator provides a flexible framework for decision-making by accommodating different attitudes, from optimistic to pessimistic. This strategy effectively manages uncertainty in node positions and subsequently focuses on minimizing energy consumption.

### III. SYSTEM MODEL

This section describes the network operation, aiming to define the architecture, the general assumption on the mobility of nodes, the propagation channel, and the detection scheme.

#### A. NETWORK ARCHITECTURE AND NODES MOBILITY

We target a network composed of  $N$  devices, typically IoT nodes, called SUs, that move over a bounded square area of side  $S$ , simulating a smart farm. The FC is placed at the center position, and a PU is located outside of the field, as depicted in Fig. 1. The distance from the  $j$ -th SU,  $j = \{1, 2, \dots, N\}$ , to both FC and PU is denoted as  $d_j^{FC}$  and  $d_j^{PU}$ , respectively. Sensor nodes handle the spectrum scarcity problem by detecting vacant frequency bands and avoiding interference with PU signal. SUs cooperate to determine the channel status by transmitting their local spectrum sensing information to FC, which aggregates the collected data to make decisions about the availability of spectrum bands.

## B. PROPAGATION CHANNEL

The wireless channel is modeled by the complex-valued channel coefficient expressed as [38]

$$h_j = \sqrt{G(d_j^{PU})} \tilde{h}_j, \quad \forall j = \{1, 2, \dots, N\}, \quad (1)$$

where  $G(d_j^{PU})$  accounts for the large-scale fading, including distance-dependent path loss and shadowing, with  $d_j^{PU}$  denoting the random distance between the  $j$ -th SU and PU (due to the random mobility of SUs). The parameter  $\tilde{h}_j$  is a standard complex Gaussian random variable describing the small-scale fading due to multi-path propagation. We use a log-distance path loss model to capture power falloff versus distance along with the random attenuation caused by the shadowing effect [38]. The path loss model, in the units of dB, reads

$$PL(d_j^{PU}) = 10\eta_j \log_{10} d_j^{PU} + X_k + X_\psi, \quad (2)$$

where  $PL(d_j^{PU}) = -G(d_j^{PU})$  dB,  $\eta_j$  is the path loss exponent,  $X_k = 10 \log_{10} (\frac{\lambda}{4\pi d_0})^2$  is the free-space path gain at reference distance  $d_0 = 1$  m and assuming omnidirectional antennas,  $\lambda$  is the wavelength, and  $X_\psi \sim \mathcal{N}(0, \sigma_{X_\psi}^2)$  is a Gaussian random variable which models the shadowing effect.

## C. DETECTION SCHEME

Each sensor detects available spectrum bands using the energy detector. We make this selection as it results in less energy consumption due to its low complexity [39]. The system operates under the parameters given by the spectrum sensing duration  $\delta$  and the sampling frequency  $f_s$ , yielding a total of processed samples as  $\delta f_s$ . Statistical decision is made by two hypothesis:  $\mathcal{H}_1$  and  $\mathcal{H}_0$  where  $\mathcal{H}_1 : y_j[n] = h_j[n]x_j[n] + u_j[n]$  represents a busy channel due to the presence of PU and  $\mathcal{H}_0 : y_j[n] = u_j[n]$  represents an idle channel due to the absent of PU. The parameter  $n = \{1, 2, \dots, \delta f_s\}$  is the time index,  $x_j[n]$  is the signal transmitted from PU,  $u_j[n]$  is an i.i.d. Gaussian noise with zero mean and variance  $\sigma_{u_j}^2$ , and  $h_j[n]$  is the channel gain between each sensor node and PU.

Local detection results have been evaluated based on decision rules about PU activity stated as:  $\mathcal{H}_1$  if  $\mathcal{E}_j \geq \epsilon$  or  $\mathcal{H}_0$  if  $\mathcal{E}_j < \epsilon$ . The term  $\epsilon$  is the detection threshold and  $\mathcal{E}_j$  is the energy of the received signal at the  $j$ -th sensor given by  $\mathcal{E}_j = \frac{1}{\delta f_s} \sum_{n=1}^{\delta f_s} |y_j[n]|^2$ . With the energy detector, the probabilities of false alarm and detection for the  $j$ -th sensor are defined as follows [39]:

$$P_{f_j} = P(\mathcal{E}_j > \epsilon | \mathcal{H}_0) = Q\left(\frac{\frac{\epsilon}{\sigma_{u_j}^2} - \delta f_s}{\sqrt{2\delta f_s}}\right), \quad (3)$$

$$P_{d_j} = P(\mathcal{E}_j > \epsilon | \mathcal{H}_1) = Q\left(\frac{\frac{\epsilon}{\sigma_{u_j}^2} - \delta f_s (\gamma_j + 1)}{\sqrt{2\delta f_s (2\gamma_j + 1)}}\right), \quad (4)$$

where  $\gamma_j = p_t |h_j|^2 / \sigma_{u_j}^2$  accounts for the SNR between  $j$ -th SU and PU,  $p_t$  is the transmission power, and  $Q$

is the complementary distribution function of the standard Gaussian distribution given by  $Q(x) = \frac{1}{\sqrt{2\pi}} \int_x^\infty e^{-\frac{t^2}{2}} dt$ .

Upon local detection, each node sends one bit to FC node to inform its local sensing result, and FC performs a combined decision with a fusion rule. In this work, we adopt the OR rule to merge the information in FC since it demonstrates superior energy efficiency for IoT networks [40]. By this rule, a given frequency band is considered occupied if at least one sensor node claims the presence of PU. Otherwise, the frequency band is free for transmissions. The resulting global probability of false alarm  $P_F$  and detection  $P_D$  are given as follows [41]:

$$P_F = 1 - \prod_{j=1}^N (1 - \rho_j P_{f_j}), \quad (5)$$

$$P_D = 1 - \prod_{j=1}^N (1 - \rho_j P_{d_j}), \quad (6)$$

considering  $\rho_j \in \{0, 1\}$ , where  $\rho_j = 1$  indicates that the  $j$ -th sensor node participates in spectrum sensing, otherwise  $\rho_j = 0$ .

We remark that the global  $P_D$  in (6) depends on the local probability of detection  $P_{d_j}$ , which is a function of the SNR and is dependent on the squared magnitude of the channel coefficient  $h_j$ . Consequently,  $P_D$  is related to the distance through the large-scale fading  $G(d_j^{PU})$ , which takes into account the mobile position of nodes in dynamic environments.

## IV. PROBLEM FORMULATION

This work focuses on determining the appropriate number of nodes participating in spectrum sensing tasks to reduce energy consumption in dynamic environments. The energy consumption model comprises three quantities reflecting the main steps in CSS to find transmission opportunities. We decompose the total energy on each SU node accounting for sensing tasks (denoted as  $E_{s_j}$ ), reporting the local detection results to FC (denoted as  $E_{t_j}$ ), as well as reporting the SU's position (denoted as  $E_{p_j}$ ). In total, the energy metric is readily given as:

$$E_T = \sum_{j=1}^N \rho_j (E_{s_j} + E_{t_j} + E_{p_j}), \quad (7)$$

where  $\rho_j \in \{0, 1\}$  indicates which nodes will be ON or OFF. The parameter  $E_{s_j}$  is considered constant for all sensors, while  $E_{t_j}$  and  $E_{p_j}$  are defined as,

$$E_{t_j} = E_{\text{elec}} + e_{\text{amp}} (d_j^{FC})^2, \quad (8)$$

$$E_{p_j} = 2n_b E_{t_j}, \quad (9)$$

where  $E_{\text{elec}}$  stands for the energy dissipated to run the radio electronics,  $e_{\text{amp}}$  is the required power amplification, and  $d_j^{FC}$  is the distance between the  $j$ -th sensor node and FC. The energy to report the positions of nodes is here a function of the number of precision bits  $n_b$  used to represent

the  $(x, y)$  coordinates. Also, the energy formulation in (7) will be stochastic-based provided each node follows random movement patterns, and it must be remarked that  $d_j^{FC}$  is a random variable as well.

To optimally reduce network energy consumption, we state a stochastic formulation problem to properly select those sensor nodes that will be ON or OFF. The network must also operate to fulfill performance metrics accounting for spectrum sensing. We assume the network should perform with an upper bound on the probability of false alarm and a lower bound on the probability of detection. Following these assumptions, the problem formulation is stated as follows:

$$\min_{\rho_j} E_T(\rho_j, d_j^{FC}) \quad (10)$$

$$\text{s.t. } P_F \leq \alpha \quad (10a)$$

$$P_D(d_j^{PU}) \geq \beta \quad (10b)$$

$$\rho_j \in \{0, 1\}, \quad (10c)$$

where the decision variable  $\rho_j$  is a binary parameter,  $d_j^{FC}$  and  $d_j^{PU}$  are random variables accounting for distances from  $j$ -th SU to FC and PU, respectively. The constraints regarding false alarm and detection global probabilities must satisfy the threshold parameters  $\alpha \in [0, 1]$  and  $\beta \in [0, 1]$ , respectively. The feasible solution to this problem is represented by the  $N$ -column vector  $\boldsymbol{\rho} = [\rho_j]$  for which the random variable  $E_T(\rho_j, d_j^{FC})$  is minimized while simultaneously guaranteeing constraints on detection performance.

## V. SENSOR SELECTION STRATEGY UNDER IGNORANCE

Solving the optimization problem posed in (10) requires previously determining the values of unknown  $d_j^{FC}$  and  $d_j^{PU}$ . These distances are related to each other and are associated with the energy metric (as in (8)) and probability of detection (as in (10b)), respectively. To solve this problem, we propose to find representative deterministic values for  $d_j^{FC}$  and  $d_j^{PU}$ , in this way to transform the stochastic formulation in (10) into a deterministic one.

We select such representative values with the OWA operator, denoted as  $F_Q$ . This operator provides a unifying framework for modeling uncertainty, allowing us to deal with the ignorance of SUs' position [23]. Using this operator, we select a representative location for each SU in the network based on the distance range and assumptions on their most likely knowledge, denoted with the function of the distance  $f$ . We denote this operation as

$$d_j = F_Q([d_{\min_j}, d_{\max_j}], f), \quad (11)$$

when transforming the distance range  $[d_{\min_j}, d_{\max_j}]$  into the representative value  $d_j$  and with  $f$  as a function parameter.

Applying the OWA operator, as presented in (11), to all distances from SUs to FC and PU enables the establishment of positions for network nodes, thereby managing uncertainty. Consequently, the stochastic optimization problem introduced in (10) can be transformed into an equivalent

deterministic formulation as follows:

$$\min_{\rho_j} E_T(\rho_j, F_Q([d_{\min_j}^{FC}, d_{\max_j}^{FC}], f)) \quad (12)$$

$$\text{s.t. } P_F \leq \alpha \quad (12a)$$

$$P_D(F_Q([d_{\min_j}^{PU}, d_{\max_j}^{PU}], f)) \geq \beta \quad (12b)$$

$$\rho_j \in \{0, 1\}, \quad (12c)$$

where both uncertain distances, contained in (12) and (12b), will be determined by mapping each interval  $[d_{\min_j}^{FC}, d_{\max_j}^{FC}]$  and  $[d_{\min_j}^{PU}, d_{\max_j}^{PU}]$  into a representative single value for  $d_j^{FC}$  and  $d_j^{PU}$ , respectively. This formulation raises an obvious question regarding the selection of values within each interval when making decisions under uncertainty about the mobility model of devices. The following sections provide further details regarding the determination of this value.

## A. TACKLING UNCERTAINTY MANAGEMENT

The selection of representative distances is evaluated from subjective and objective standpoints [23]. The subjective standpoint refers to the decision-maker attitude, also known as the attitudinal character, assessed through a basic unit-interval monotonic (BUM) function denoted as  $Q(y)$ . The objective knowledge, typically partial knowledge about the mobility model, is defined by the likely distance function  $f$ , which evaluates the most probable distances. It is noteworthy that the functions  $Q(y)$  and  $f$  can have multiple definitions in accordance with the network scenario and SU mobility models. Further details on these functions consistent with IoMT scenarios are provided in the subsequent subsections. The OWA operator is defined as:

$$F_Q([d_{\min}, d_{\max}], f) = \int_0^1 \frac{dQ(y)}{dy} H^{-1}(y) dy, \quad (13)$$

where

$$H(x) = \int_x^{d_{\max}} g(z) dz, \quad (14)$$

and

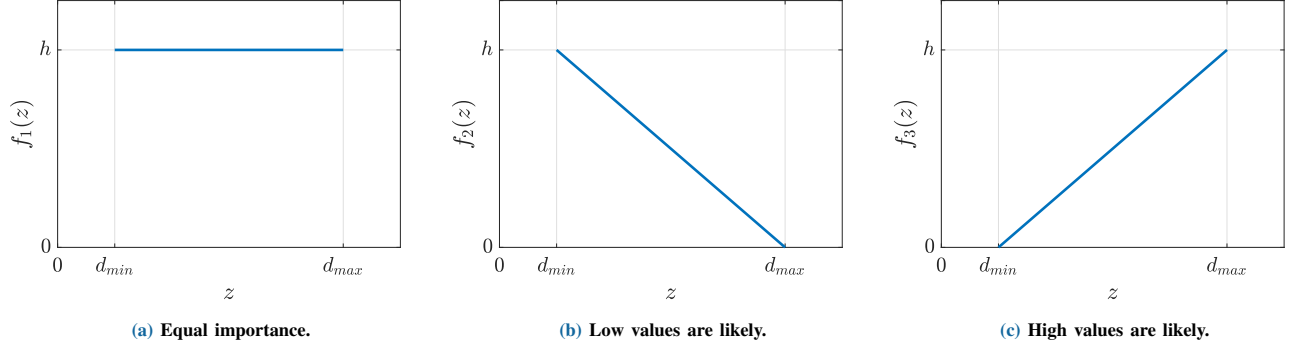
$$g(z) = \frac{f(z)}{\int_{d_{\min}}^{d_{\max}} f(x) dx}, \quad (15)$$

where the monotonic function  $Q : [0, 1] \mapsto [0, 1]$  satisfies  $Q(0) = 0$ , and  $Q(1) = 1$ .

In this paper, we use a polynomial function to define  $Q$  as  $Q(y) = y^p$  [23] as it provides a straightforward interpretation for the OWA operator with the parameter  $p$ ; see Section 1. As for the function  $f$ , we discuss three variants while assuming more likely distance sub-ranges than others; see Section 2.

### 1) SOLVING FOR THE ATTITUDINAL CHARACTER

The function  $Q$  captures the subjective belief of the decision-maker regarding the location of nodes. Using  $Q(y) = y^p$  for all  $p \geq 0$  implicitly define an attitudinal character as for the solution in (13). This is a mathematically tractable function and illustrates a wide range of judgments. For instance, if we consider the function  $f(z) = K$ , where  $K$  is a constant


**FIGURE 2: Importance of weights contained in the function  $f(z)$ .**

describing equal importance for all possible distances inside the interval, we obtain the following solution

$$F_Q([d_{\min}, d_{\max}], K) = \frac{d_{\max} + pd_{\min}}{p+1}, \quad (16)$$

after evaluating these two functions in (13), where the value of  $p$  will directly define a representative distance between the optimistic and pessimistic attitudes. The decision attitude is reduced to setting the value of  $p$  according to a subjective belief about the nodes' position over the simulation scenario. If we believe that nodes are close to the edge of the area ( $d_{\max}$ ), we make  $p \rightarrow 0$ . This is a pessimistic attitude as it evaluates the greatest energy consumption. On the contrary, if we expect that the devices are around the center ( $d_{\min}$ ), we set  $p \rightarrow \infty$ . This evaluates an optimistic attitude as it defines the least possible energy consumption. The interval average is modeled by choosing  $p \rightarrow 1$ , which stands for an arbitrary decision-maker attitude.

## 2) SOLVING WITH PARTIAL KNOWLEDGE ABOUT THE MOBILITY MODEL

The objective partial knowledge of the mobility model can be introduced by employing various functions for  $f$ . The function  $f$  will influence the decision of the distances  $d_j^{FC}$  and  $d_j^{PU}$  when solving for the OWA operator in (13). We do not assume any exact knowledge about their statistical distributions, but we can describe which values, or ranges of values, are more important or more likely [42]. Three intuitive ways allow capturing the realizations of the distances from each SU to FC and PU as depicted in Fig. 2.

The first one, depicted in Fig. 2a, describes the evenly distributed weights due to no objective information, and the subjective attitude of the decision-maker will prevail. However, for a given position of FC and PU, the mobility patterns of SUs could lead us to identify that shorter or longer distances  $\{d_j^{FC}, d_j^{PU}\}$  tend to predominate. In such a case, it is fair to define decreasing functions as shown in Fig. 2b when lower values are more critical or increasing functions as depicted in Fig. 2c if larger values are more probable. Although the actual movement patterns of devices

are unknown, the choice of these functions  $f$  seeks to recreate uniform behavior or extreme cases that illustrate possible situations.

Closed-form expressions for the functions  $f(z)$  are given below considering the parameter  $h$  is a constant that vanishes after the normalization shown in (15):

$$f_1(z) = K, \quad (17)$$

$$f_2(z) = -\frac{h}{d_{\max} - d_{\min}}z + \frac{hd_{\max}}{d_{\max} - d_{\min}}, \quad (18)$$

$$f_3(z) = \frac{h}{d_{\max} - d_{\min}}z - \frac{hd_{\min}}{d_{\max} - d_{\min}}, \quad (19)$$

where  $f_1(z), f_2(z), f_3(z)$  are non-negative functions reflecting the importance associated with the value  $z \in [d_{\min}, d_{\max}]$ . In particular, let us consider the case where  $f(z)$  is linear with a negative slope, leading to  $f(z) = f_2(z)$ , as exposed in Fig. 2b. Substituting in (13) and solving for  $Q(y) = y^p$ , a solution arises as a function of the exponent  $p$  similar to equal-importance weights approach as:

$$F_Q([d_{\min}, d_{\max}], f_2) = d_{\max} - (d_{\max} - d_{\min})\frac{2p}{2p+1}. \quad (20)$$

It can be noticed that when  $p \rightarrow 0$ , we get the maximum distance  $d_{\max}$ , and when  $p \rightarrow \infty$ , we get the minimum distance  $d_{\min}$ . Another interesting result emerges when  $p \rightarrow 1$ , then the operator yields  $(d_{\max} + 2d_{\min})/3$  instead of the average as in the case of  $f_1(z) = K$ .

We analyze the opposite situation for a function  $f(z)$  that has a positive slope, yielding  $f(z) = f_3(z)$ , as shown in Fig. 2c, in this way introducing more weight into the higher distance range. Solving (13) for the same function  $Q(y) = y^p$  and after some mathematical modifications, we get:

$$F_Q([d_{\min}, d_{\max}], f_3) = d_{\min} + (d_{\max} - d_{\min})I(y), \quad (21)$$

where

$$I(y) = \int_0^1 py^{p-1}(1-y)^{\frac{1}{2}} dy, \quad (22)$$

which does not evaluate a closed-form expression and must be solved numerically. We discuss its evaluation in the next section.

Unfortunately, we can not directly apply OWA to determine distances  $d_j^{FC}$  and  $d_j^{PU}$  because of geometric constraints which prohibit the selection of some values to indicate every sensor location. The position of each SU is associated with a distance to FC that fixes the set of distances to PU or vice versa. For instance, an adequate spatial coordinate for a SU may not coincide with the longest or shortest distance to FC and PU for such a scenario, as shown in Fig. 1.

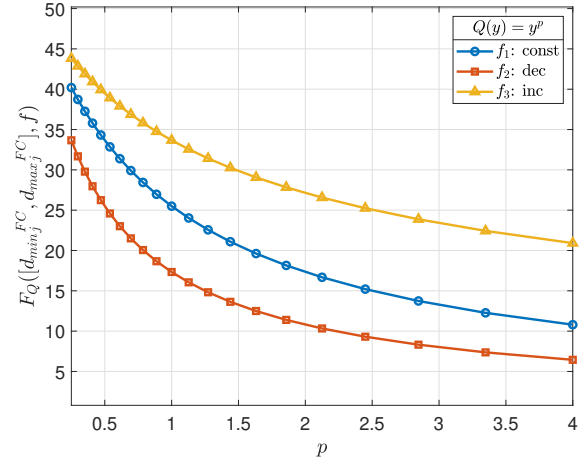
## B. ENERGY OPTIMIZATION FOR HOMOGENEOUS DECISIONS

To solve the optimization problem presented in (12), we can use a homogeneous approach where equal strategy is applied to each SU (subjective and objective in Section 1 and 2). In simple terms, a single pair  $(d_j^{FC}, d_j^{PU})$  is taken as a representative position for all SUs in the entire network. This approach emulates under-risk solutions where each node has the same statistical features provided by a standard mobility model.

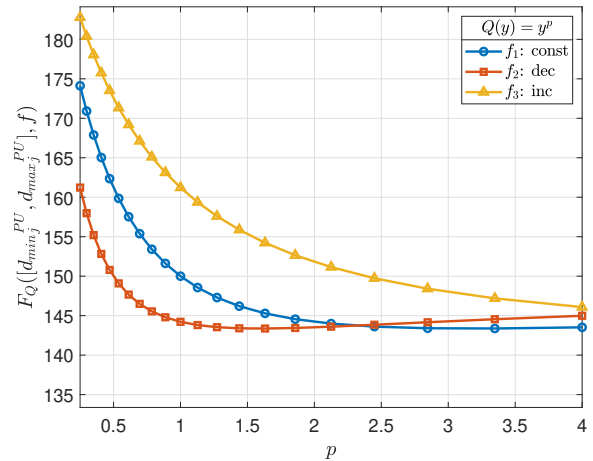
A methodology to solve the problem in (12) will first find the representative values for  $d_j^{FC}$  and  $d_j^{PU}$  and then solve the problem to find which nodes will be ON and OFF. The methodology is detailed as follows:

- (i) Determine the interval  $[d_{\min}^{FC}, d_{\max}^{FC}]$  accounting for the distance range between SUs and FC node. For instance, in the grid depicted in Fig. 1,  $d_j^{FC} \in [1, \frac{\sqrt{2}}{2}S]$  as we consider a square grid with granularity the unit and maximum width of  $S$  units.
- (ii) Evaluate the OWA operator using Equations (16), (20) or (21) to choose a representative value for  $d_j^{FC}$  in the interval  $[d_{\min}^{FC}, d_{\max}^{FC}]$ .
- (iii) Find the distance range  $[d_{\min}^{PU}, d_{\max}^{PU}]$  between SUs and PU node. For instance, the fixed  $d_j^{FC}$  will sketch a circle where the solution is located. The minimum distance  $d_{\min}^{PU}$  will be defined as the point on the circle that is closest to PU, and the maximum distance  $d_{\max}^{PU}$  will be defined as the point on the circle that is farthest from the PU. To identify both points, we readily find the interceptions between a line passing through the FC and PU positions and the circle, as depicted in Fig. 1.
- (iv) Evaluate the OWA operator using Equations (16), (20) or (21) to choose a representative value for  $d_j^{PU}$  in the interval  $[d_{\min}^{PU}, d_{\max}^{PU}]$ .
- (v) Solve the optimization problem posed in (12) to minimize the energy consumption.

To illustrate, Fig. 3 shows the solution for the OWA operator following the steps (i) to (iv). The evaluation in Fig. 3a and Fig. 3b involves the assessment of the representative scores for the distances from SU to FC and PU, designated as  $d_j^{FC}$  and  $d_j^{PU}$ , respectively. All curves are obtained employing the same attitude function as  $Q(y) = y^p$  for distinct values of  $p$ , and three assumptions on the movement



(a) Representative  $d_j^{FC}$  values.



(b) Representative  $d_j^{PU}$  values.

FIGURE 3: Different objective and subjective decisions over an area of side  $S = 100$  m.

of nodes  $\{f_1(z), f_2(z), f_3(z)\}$  as stated in (17), (18), (19). The length of the square area is  $S = 100$  m, FC is located at the center, and PU is outside to the right of the simulation area. The results validate that the maximum is reached when  $p \rightarrow 0$ , and the representative distance decreases with  $p$ . In addition, for a given  $p$  value, higher outcomes are shown for the increasing, constant, and decreasing functions  $f(z)$  in that order, except for the second distance  $d_j^{PU}$ . This interval depends on the previous decision about  $d_j^{FC}$ , which varies from one function  $f(z)$  to another.

The feasible solution to the optimization problem in (12) can be addressed following the homogeneous decision approach. A single pair of distances  $\{d_j^{FC}, d_j^{PU}\}$  will represent the whole set of potential combinations. The approximate amount of sensors with  $\rho_j = 1$  can be derived by simply activating the requisite number of sensors to fulfill the

detection constraint in (12b), with the remaining sensors entering a sleep mode to conserve energy.

### C. ENERGY OPTIMIZATION FOR HETEROGENEOUS DECISIONS

The preceding section shows an extreme case when a single pair  $(d_j^{FC}, d_j^{PU})$  models all nodes' positions. A more general situation can be addressed when levels between the optimistic and the pessimistic cases are equipartitioned among nodes, referred to as a heterogeneous approach. Under this consideration, the decision-maker has to make  $N$  selections for the expected positions of sensors. We define two terms: a continuous random variable uniformly distributed  $X_p \sim \mathcal{U}(p_{\min}, p_{\max})$  accounting for the exponent of the attitudinal function  $Q(y)$ , and the set  $f_i(z) = \{f_1(z), f_2(z), f_3(z)\}$  representing the knowledge about the distribution of distances, where we model the member index  $i$  as a discrete random variable uniformly distributed  $i \sim \mathcal{U}\{1, 3\}$ . Thus, we can model a heterogeneous scenario using the observed values of two random variables to obtain specific distances  $d_j^{FC}$  and  $d_j^{PU}$  for each SU.

Next, we can find the minimum number of awake nodes based upon the OWA-dependent optimization problem in (12). Firstly, we execute steps (i) to (iv) in Section B for each  $j$ -th sensor node,  $j = \{1, 2, \dots, N\}$ . Lastly, we find the optimal solution to reduce energy consumption via (v).

To simplify the solution for the non-convex problem stated in (12), we adopt the method outlined in [11]. Initially, we modify the constraint in (12a) because  $P_F$  is independent of PU signal. This change imposes an upper bound for the total number of active nodes. We have also revised the domain of  $\rho_j$  to remove the binary constraint, leading to a relaxed problem denoted as:

$$\min_{\rho_j} E_T(\rho_j, F_Q([d_{\min_j}^{FC}, d_{\max_j}^{FC}], f)) \quad (23)$$

$$\text{s.t.} \quad \sum_{j=1}^N \rho_j \leq \left\lfloor \frac{\ln(1-\alpha)}{\ln\left(1 - Q\left(\left(\frac{\epsilon}{\sigma_{u_j}^2} - 1\right)\sqrt{\delta}f_s\right)\right)} \right\rfloor = M \quad (23a)$$

$$P_D(F_Q([d_{\min_j}^{PU}, d_{\max_j}^{PU}], f)) \geq \beta \quad (23b)$$

$$\rho_j \in [0, 1]. \quad (23c)$$

Solving for (23), we can analyze the first-order partial derivative condition for the Lagrangian function by finding the stationary points. However, this requires solving an equation system involving  $N$  unknown variables  $\rho_j$ , which can be computationally expensive. To tackle this concern, we derive a cost function per  $j$ -th sensor node that quantifies its level of preference compared to the other nodes, formulated as:

$$C_j = E_{s_j} + (1 + n_b)(E_{\text{elec}} + e_{\text{amp}}(d_j^{FC})^2) - \lambda P_{d_j}, \quad (24)$$

to determine which nodes will be ON or OFF. This cost function represents a priority metric to identify the nodes with

---

#### Algorithm 1: OWA-Based Sensor Selection

---

**Input:**  $N, S$

**Output:**  $\rho, E_T$

```

1 nodes = 1,  $\lambda_{\min} = 0, \lambda_{\max} = \zeta, \epsilon$  is a small enough
  number,  $\rho[1 : N] \leftarrow 0, M$  based on (23a)
2 while  $|\lambda_{\max} - \lambda_{\min}| > \epsilon$  do
3    $\lambda = (\lambda_{\max} + \lambda_{\min})/2$ 
4   for  $j = 1$  to  $N$  do
5     Observed values:  $X_p \rightarrow Q, i \rightarrow f_i$ 
6      $d_j^{FC} \leftarrow F_Q([d_{\min_j}^{FC}, d_{\max_j}^{FC}], f_i)$ 
7      $d_j^{PU} \leftarrow F_Q([d_{\min_j}^{PU}, d_{\max_j}^{PU}], f_i)$ 
8      $P_{d_j}(d_j^{PU})$  based on (4)
9      $C_j$  based on (24);
10  Rearrange  $C_j$  in ascending order and store
  indexes
11  while nodes  $\leq M$  do
12     $\rho[\text{nodes}] \leftarrow 1$ 
13     $P_D(F_Q([d_{\min_j}^{PU}, d_{\max_j}^{PU}], f_i))$  for nodes
14    if  $P_D \geq \beta$  then
15      break
16    nodes  $\leftarrow$  nodes + 1
17  if  $P_D \geq \beta$  then
18     $\lambda_{\max} \leftarrow \lambda$ 
19  else if  $P_D < \beta$  then
20     $\lambda_{\min} \leftarrow \lambda$ 
21   $E_T$  for nodes

```

---

the lowest energy consumption and the highest probability of detection. The first two terms in (24) account for the energy metric, while the last term indicates the detection capability of nodes. Using this metric, nodes with the lowest  $C_j$  value will be chosen to be in ON mode, ensuring compliance with the constraints in (23a) and (23b).

We summarize the main steps of the approximate solution with the pseudocode in Algorithm 1. The pseudocode comprises two blocks mainly, one block to evaluate the representative distances with the OWA operator and compute the cost functions with (24), and a second block to select the nodes in the ON state. The first line initializes the required variables, followed by a preprocessing stage (lines 3 to 10), which decides nodes' positions based on the OWA operator and evaluates the cost function. The selection stage (lines 11 to 21) seeks appropriate nodes to participate in spectrum sensing and updates the search space of the Lagrange multiplier  $\lambda$  (line 18 or 20).

The time complexity of Algorithm 1 is the result of three phases: *while* loop in line 2 that executes a binary search with  $O(\log \zeta)$  where  $\zeta$  accounts for the maximum number of Lagrange multiplier; a second *while* loop in line 11 where  $M$  is upper bounded by  $N$ , thereby obeying to  $O(N)$ ; and last, the line 13 computes  $P_D$  for  $N$  nodes in the worst-case scenario such that implies  $O(N)$ . By combining



all stages, we obtain a time complexity of  $O(N^2 \log \zeta)$ . However, a fixed value of  $\zeta > 0$  could be derived, as suggested in [11], to reduce the search space and transform the time complexity of the main loop into constant  $O(1)$ . As a result, the time complexity of our solution can be reduced to  $O(N^2)$ , surpassing the time complexity of the exhaustive search algorithm  $O(N!)$ . Remarkably, the proposed solution does not incur additional data transmission to determine the ON/OFF state of network nodes, thereby resulting in negligible communication overhead.

## VI. PERFORMANCE EVALUATION

This section presents the simulation results for both strategies: homogeneous and heterogeneous. The energy efficiency is initially examined for different approaches based on subjective attitudinal character and objective knowledge of the SU mobility. Then, we explore the implications of adopting specific mobility models, such as Random Waypoint and Gauss-Markov, to describe movement patterns. We highlight how our proposed solution aligns with these patterns, even under complete ignorance. The selection of mobility patterns is motivated by their relevance in modeling ground user behavior within contemporary drone-assisted networks, as demonstrated in [43], [44]. This simulation environment aligns with potential applications of mobile networks in IoMT, as previously discussed in the context of smart agriculture. In such scenarios, nodes must share the spectrum resources available for transmissions while reducing energy consumption.

It is worthwhile noting that our solution applies following the perspective of a “wait-and-see” approach, which identifies the optimal number of awake nodes in each time slot. In this case, we implement the energy efficient sensor selection (EESS) algorithm to discuss the boundaries of our proposal [11]. In addition, we conduct comparisons with “here-and-now” approaches, which previously estimate the statistical features of distances as in [21], [22]. The simulation scenarios are examined for various network sizes,

corresponding to the density of SUs per square meter for a fixed number of nodes, and with FC positioned at the center of the field.

Table 1 outlines the parameters utilized in numerical simulations unless explicitly specified otherwise. The values for energy consumption were obtained from the 2.4 GHz RF Transceiver CC2500 datasheet by Texas Instruments [45]. The energy wasted in sensing tasks  $E_{s_j}$  is derived by adding a typical value of 40 nJ used for the receiving electronic components and the energy involved in the signal processing phase of 153 nJ. The energy terms associated with the transmission of sensing results to FC are  $E_{elec} = 80$  nJ and  $e_{amp} = 40.4$  pJ/m<sup>2</sup> similar to [46]. The parameter  $E_{p_j}$  is only considered by the “wait-and-see” algorithm because SUs must update their positions to FC to perform the sensors selection. For the  $(x, y)$  coordinates of each SU transmitted to FC, we assume a precision of  $n_b = 8$  bits.

### A. IMPACT OF PARAMETERS

Fig. 4 illustrates a variety of scenarios through the proposed OWA operator with the optimistic and pessimistic approaches. Both the number of active nodes and the corresponding energy consumption value tend to decrease with the increase of  $p$ , despite the knowledge about nodes’ distribution in the grid, given by the function  $f(z)$ . In addition, our understanding of movement rules with  $f(z)$  leads to establishing distinct levels of active nodes and energy expended. For instance, assuming that SUs will be more likely apart from FC and PU nodes (function  $f_3(z)$ ), will accordingly require the more significant energy consumption in the network compared to the opposite behavior with the function  $f_2(z)$ , where we assume the lowest distance. In the following sections, we aim to find appropriate combinations of  $Q(y)$  and  $f(z)$  functions suitable for realistic scenarios applicable to femtocells in mobile networks [47].

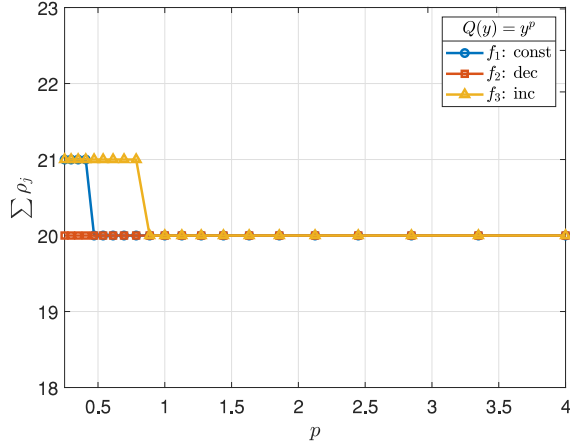
### B. ASSESSING RISK AND IGNORANCE APPROACHES

To evaluate decision-making under risk and ignorance, we distribute  $N = 100$  sensors over a square area of side  $S$  in the range 50 m to 100 m, and implement mobility with two cases: Random Waypoint and Gauss-Markov mobility models. With this simulation, we can accurately evaluate the statistical moments and the PDF of distances from every SU to FC and PU, which provides a way to interpret our proposed solution. We also compare decision-making under ignorance to certainty and risk-based approaches.

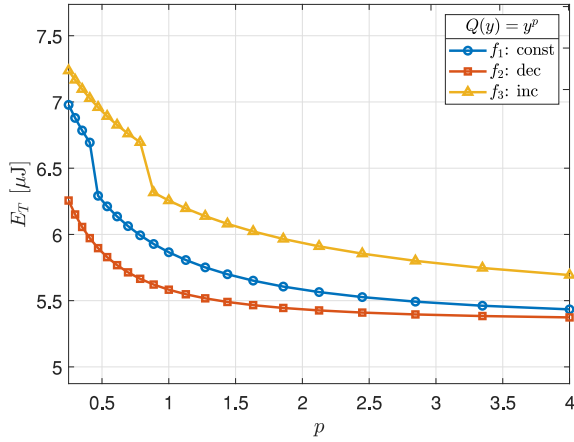
Fig. 5 compares the energy consumption with the Random Waypoint mobility model and uses the OWA operator to estimate distances from SUs to FC and PU. The comparisons include the expected values of distances (labeled as ‘mean rway’ [21]), the expected values plus  $k$  times the standard deviation (labeled as ‘mean-std rway’ [21]), and a bounded energy value with a probability  $\theta$  (labeled as ‘kataoka rway’ [22]). Setting the parameter  $k = 10$  and  $\theta = (1 - \frac{1}{k}) = 0.9$  ensures that energy values remain within the predefined

TABLE 1: Parameters values in the system model.

Parameter	Value
Number of nodes, $N$	100
Side length of the network area, $S$	50 m to 100 m
Transceiver frequency, $f_c$	2.4 GHz
Transmission power, $p_t$	20 mW
Bandwidth, $B$	1 MHz
Noise power spectrum density, $N_0$	-170 dBm/Hz
Noise power, $\sigma_{u_j}^2 = N_0 B$	-110 dBm
Probability of detection threshold, $\beta$	0.9
Probability of false alarm threshold, $\alpha$	0.1
Energy of sensing tasks, $E_{s_j}$	193 nJ
Energy dissipated, $E_{elec}$	80 nJ
Power amplification, $e_{amp}$	40.4 pJ/m <sup>2</sup>
Bits used to report the SU position, $n_b$	8 bits



(a) Total awake nodes.



(b) Energy consumption.

FIGURE 4: Homogeneous approach outputs for an area of  $S = 100$  m.

interval and that the upper bound on energy is minimized with the same probability.

Our solution for homogeneous decisions using  $Q(y) = y^4$  and  $f_1(z)$  is similar to the expected value approach with a root mean square error (RMSE) of  $1.17 \mu\text{J}$ , as shown in Fig. 5. Furthermore, the statistical characteristics of both distances  $d_j^{FC}$  and  $d_j^{PU}$  are not required to determine the optimal number of active nodes, which represents one of the primary advantages of our proposal. Also, for  $f_3(z)$  and the same attitude  $Q(y)$ , the shape of the energy curve fits the Kataoka approach with an RMSE of  $0.33 \mu\text{J}$ . Furthermore, the function  $f_2(z)$  leads to an over-optimistic outcome, which may not satisfy the lower bound of energy or detection constraints.

To avoid over-optimistic cases, we compare the energy consumption of the proposed method with the average of the EESS static algorithm, which provides the optimal solution in each time slot. To be more general, we assume that all nodes move following the Gauss-Markov mobility model,

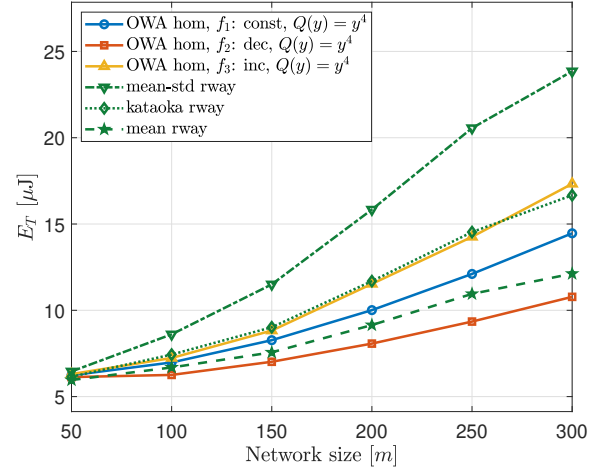


FIGURE 5: Energy consumption compared to under risk approaches for devices with a Random Waypoint mobility model.

a memory system that provides more realistic movement patterns. The two extreme cases for this mobility model are displayed with black color lines in Fig. 6. Both curves expose the optimal energy wasted with and without exchanging information regarding the positions of SUs. Specifically, the worst-case, shown with a solid line, is considerably far away from the other curves provided that  $E_{p_j}$  must be included in the energy formulation. The ideal case represented by a dotted line is derived by omitting the  $E_{p_j}$ . Any curve between the ideal and the worst case is a valid solution to the original problem.

In addition, Fig. 6 includes the homogeneous decisions with  $Q(y) = y$  and the three options for  $f(z)$ , and the heterogeneous decisions regarding the position of each SU. The plot for function  $f_2(z)$  with decreasing slope has energy values below the lower bound. We adopt a conservative attitude to amend this issue, selecting a value of  $p < 1$ . For instance, the dash-dotted red line depicts the function  $Q(y) = y^{\frac{2}{3}}$  that fulfills the energy requirements. Surprisingly, the energy behavior of the heterogeneous approach, shown in the violet color, is similar to that of the conservative homogeneous decision. The RMSE values for homogeneous and heterogeneous decisions with respect to the energy lower bound are  $0.49 \mu\text{J}$  and  $0.67 \mu\text{J}$ , respectively. However, the heterogeneous decision approach has the advantage of being able to select the specific nodes to be activated based on an attitudinal character and a reduced knowledge about the most probable distances  $d_j^{FC}$  and  $d_j^{PU}$ .

### C. DETECTION PERFORMANCE

Finally, we account for the global probabilities of detection and false alarm,  $P_D$  and  $P_F$ , to validate the detection constraints. The transmitted PU signal is composed of a rectangular pulse train contaminated with additive white gaussian noise (AWGN) and the SNR parameter ranges

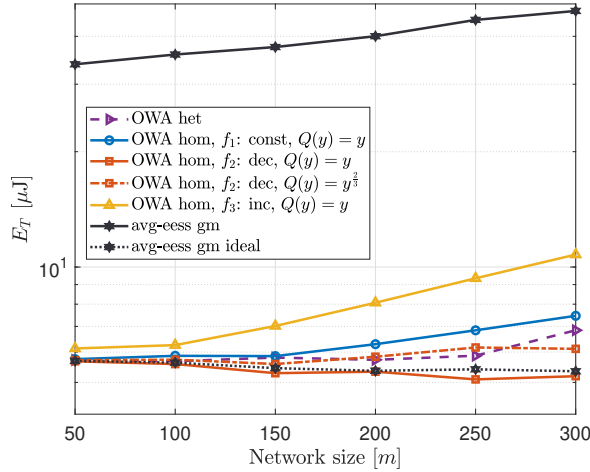


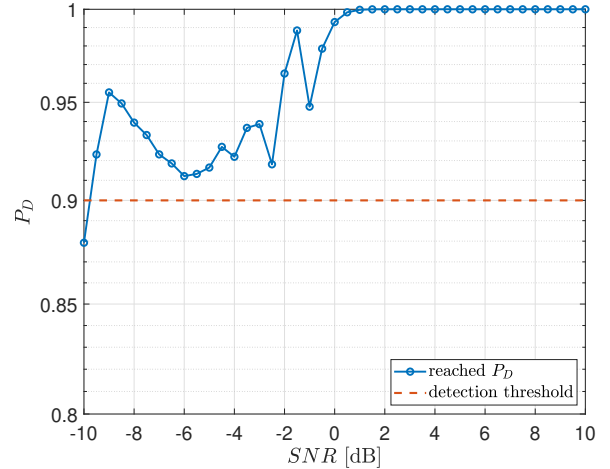
**FIGURE 6: Energy consumption for homogeneous and heterogeneous decisions compared to under certainty approach and Gauss-Markov mobility model.**

on the interval  $[-10, 10]$  dB. The number of samples per pulse is  $\delta f_s = 100$ , and the number of transmitted bits of information is  $10^6$ . We estimate the local detection and false alarm probabilities,  $P_d$  and  $P_f$  with the Monte Carlo simulation. For a given SNR value at the  $j$ -th SU, the Algorithm 1 returns the number of required nodes to fulfill detection constraints. Then, we use these values to compute the OR fusion rule and verify if  $P_D$  and  $P_F$  have been satisfied, as shown in Fig. 7.

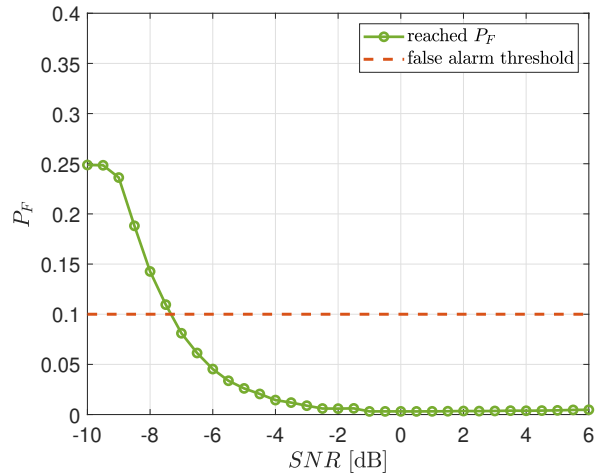
Fig. 7a demonstrates that  $P_D$  exceeds the detection threshold  $\beta = 0.9$  for  $\text{SNR} \geq -9.5$  dB avoiding interference with PU signal. This curve is monotonically increasing on those intervals where the estimated local probability of detection is growing faster than the number of active nodes, which decreases due to better SNR values. Moreover, when  $\text{SNR} = -10$  dB, it is not enough with 100 SUs to reach the detection threshold through the fusion rule. Fig. 7b depicts that  $P_F$  curve is below the threshold  $\alpha = 0.1$  for  $\text{SNR} \geq -7$  dB. The  $P_F$  curve is decreasing because fewer nodes have been selected to participate in the spectrum sensing phase. The constant interval accounts for the best case where only one SU satisfies the false alarm constraint.

#### D. REAL-WORLD IMPLICATIONS

The proposed solution presents potential avenues for implementation in wireless networks comprising battery-limited devices, including UAVs, autonomous vehicles, and mobile IoT nodes for smart cities. Regarding energy efficiency, this approach based on the OWA operator eliminates the need for devices to report their positions during CSS tasks to a controller node, such as a fixed BS in UAV-assisted networks or an roadside unit (RSU) in vehicular networks. Consequently, it saves energy by avoiding communication overhead. Regarding detection constraints, our proposal is



**(a) Global probability of detection.**



**(b) Global probability of false alarm.**

**FIGURE 7: Detection constraints for different SNR values.**

deployable for an SNR of at least  $-7$  dB. This constraint guarantees the successful identification of spectrum holes for transmissions without interfering with the PU signal. In a practical scenario like the case of beyond fifth generation (B5G) networks, it is postulated that a multitude of mobile nodes will be available for the IoT paradigm, with UAVs acting as flying BSs, which will be empowered by three-dimensional mobility. Consequently, the device characteristics will be advantageous in ensuring the required SNR for successfully detecting the PU signal.

Nevertheless, the aforementioned network scenarios could potentially support the execution of the OWA-based algorithm, albeit with certain limitations or prior modifications. The primary challenge lies in implementing a training stage to assess the efficacy of different objective and subjective standpoints for managing the uncertainty of node positions by means of functions  $f$  and  $Q$ . In this context, it is

necessary to examine alternative mobility models besides Random Waypoint and Gauss-Markov that may be more suitable for urban scenarios. Such motion patterns may include the Levy Walk, which describes human mobility [48], or group mobility models for platooning in vehicular networks [49]. Conversely, it can be argued that homogeneous decisions, where one location represents the entire set of nodes, may be more suitable for characterizing group mobility models. However, heterogeneous decisions, where each node is individually represented by a distinct location, are more appropriate for simulating movements with rapid fluctuations, such as those performed by drones.

## VII. CONCLUSION

This paper proposes a novel approach based on OWA operator for energy-aware device selection under ignorance with detection constraints in IoMT environments. We discuss two directions according to the decision strategy: homogeneous and heterogeneous. The former supposes that one spatial coordinate in the area is sufficient to represent the tendency in the positions of nodes. The latter addresses a more general case where the levels of optimism and pessimism are equipartitioned between each SU making individual decisions about their positions. Then, we find the minimum number of active nodes that must participate in spectrum sensing to reduce energy consumption. The numerical results focus on evaluating the performance of different attitudes of the decision-maker to identify the appropriate approach. The energy consumption fits stochastic decisions, considered under risk solutions, without knowledge of statistical features of movement. Also, the behavior of the proposed algorithm is bounded by the average static solution per time slot. We conclude with a set of functions  $Q$  and  $f$  suitable for nodes guided by Random Waypoint and Gauss-Markov mobility models. The global probabilities of detection and false alarm are guaranteed for  $\text{SNR} \geq -7$  dB for the simulation environment under study. The potential for developing new functions applicable to B5G network scenarios is a topic that will be addressed in the future.

## APPENDIX

### List of Acronyms

AWGN	additive white gaussian noise
B5G	beyond fifth generation
BS	base station
BUM	basic unit-interval monotonic
CSS	cooperative spectrum sensing
EESS	energy efficient sensor selection
FC	fusion center
IoMT	Internet of Mobile Things
IoT	Internet of Things
ISM	industrial, scientific, and medical
ITS	intelligent transportation systems

OWA	ordered weighted averaging
PDF	probability density function
PU	primary user
RMSE	root mean square error
RSU	roadside unit
SNR	signal to noise ratio
SU	secondary user
UAV	unmanned aerial vehicle
WSN	wireless sensor network

## REFERENCES

- [1] A. K. Singh, "Smart Farming: Applications of IoT in Agriculture," in *Handbook of Smart Materials, Technologies, and Devices: Applications of Industry 4.0*, C. M. Hussain and P. Di Sia, Eds. Cham: Springer International Publishing, 2022, pp. 1655–1687.
- [2] M. N. Mowla, N. Mowla, A. F. M. S. Shah, K. M. Rabie, and T. Shongwe, "Internet of Things and Wireless Sensor Networks for Smart Agriculture Applications: A Survey," *IEEE Access*, vol. 11, pp. 145 813–145 852, 2023.
- [3] J. Mitola and G. Q. Maguire, "Cognitive radio: making software radios more personal," *IEEE Personal Communications*, vol. 6, no. 4, pp. 13–18, Aug. 1999.
- [4] M. Ibnkahla, *Wireless Sensor Networks: A Cognitive Perspective*. CRC Press, Apr. 2016.
- [5] I. Dietrich and F. Dressler, "On the lifetime of wireless sensor networks," *ACM Transactions on Sensor Networks*, vol. 5, no. 1, pp. 1–39, Feb. 2009.
- [6] W. Lu, T. Nan, Y. Gong, M. Qin, X. Liu, Z. Xu, and Z. Na, "Joint Resource Allocation for Wireless Energy Harvesting Enabled Cognitive Sensor Networks," *IEEE Access*, vol. 6, pp. 22 480–22 488, 2018.
- [7] X. Liu, K. Zheng, K. Chi, and Y.-H. Zhu, "Cooperative Spectrum Sensing Optimization in Energy-Harvesting Cognitive Radio Networks," *IEEE Transactions on Wireless Communications*, vol. 19, no. 11, pp. 7663–7676, Nov. 2020.
- [8] M. Zheng, L. Chen, W. Liang, H. Yu, and J. Wu, "Energy-Efficiency Maximization for Cooperative Spectrum Sensing in Cognitive Sensor Networks," *IEEE Transactions on Green Communications and Networking*, vol. 1, no. 1, pp. 29–39, Mar. 2017.
- [9] J. A. Ansere, G. Han, H. Wang, C. Choi, and C. Wu, "A Reliable Energy Efficient Dynamic Spectrum Sensing for Cognitive Radio IoT Networks," *IEEE Internet of Things Journal*, pp. 6748 – 6759, 2019.
- [10] M. Najimi, "Energy harvesting, cooperative spectrum sensing, and data transmission improvement in energy-efficient multichannel cognitive sensor networks," *International Journal of Communication Systems*, vol. 32, no. 13, p. e4031, 2019.
- [11] M. Najimi, A. Ebrahimzadeh, S. M. H. Andargoli, and A. Fallahi, "A Novel Sensing Nodes and Decision Node Selection Method for Energy Efficiency of Cooperative Spectrum Sensing in Cognitive Sensor Networks," *IEEE Sensors Journal*, vol. 13, no. 5, pp. 1610–1621, May 2013.
- [12] —, "Energy-Efficient Sensor Selection for Cooperative Spectrum Sensing in the Lack or Partial Information," *IEEE Sensors Journal*, vol. 15, no. 7, pp. 3807–3818, Jul. 2015.
- [13] A. Bagheri, A. Ebrahimzadeh, and M. Najimi, "Sensor selection for extending lifetime of multi-channel cooperative sensing in cognitive sensor networks," *Physical Communication*, vol. 26, pp. 96–105, Feb. 2018.
- [14] —, "Energy-efficient sensor selection for multi-channel cooperative spectrum sensing based on game theory," *Journal of Ambient Intelligence and Humanized Computing*, vol. 12, no. 10, pp. 9363–9374, Oct. 2021.
- [15] Z. Jin, Y. Qiao, A. Liu, and L. Zhang, "EESS: An Energy-Efficient Spectrum Sensing Method by Optimizing Spectrum Sensing Node in Cognitive Radio Sensor Networks," *Wireless Communications and Mobile Computing*, vol. 2018, 11 pages, Jul. 2018.
- [16] M. Monemian, M. Mahdavi, and M. J. Omid, "Improving the lifetime of multichannel cognitive radio sensor networks via new spectrum sensing method," *Transactions on Emerging Telecommunications Technologies*, vol. 30, no. 5, 2019.

- [17] T. H. Pham, D. Ichalal, and S. Mammam, "Complete coverage path planning for pests-ridden in precision agriculture using UAV," in *2020 IEEE International Conference on Networking, Sensing and Control (ICNSC)*, Oct. 2020, pp. 1–6.
- [18] R. I. Mukhamediev, K. Yakunin, M. Aubakirov, I. Assanov, Y. Kuchin, A. Symagulov, V. Levashenko, E. Zaitseva, D. Sokolov, and Y. Amirgaliyev, "Coverage Path Planning Optimization of Heterogeneous UAVs Group for Precision Agriculture," *IEEE Access*, vol. 11, pp. 5789–5803, 2023.
- [19] X. Cai, J. Sheng, Y. Wang, B. Ai, and C. Wu, "A Novel Opportunistic Access Algorithm Based on GCN Network in Internet of Mobile Things," *IEEE Internet of Things Journal*, vol. 10, no. 13, pp. 11 631–11 642, Jul. 2023.
- [20] D. Pliatsios, S. K. Goudos, T. Lagkas, V. Argyriou, A.-A. A. Boulogeorgos, and P. Sarigiannidis, "Drone-Base-Station for Next-Generation Internet-of-Things: A Comparison of Swarm Intelligence Approaches," *IEEE Open Journal of Antennas and Propagation*, vol. 3, pp. 32–47, 2022.
- [21] K. Toledo, H. Kaschel, and J. Torres, "A stochastic approach for spectrum sensing and sensor selection in dynamic cognitive radio sensor networks," *Physical Communication*, vol. 37, p. 100879, Dec. 2019.
- [22] H. Kaschel, K. Toledo, J. T. Gómez, and M. J. F.-G. García, "Energy-Efficient Cooperative Spectrum Sensing Based on Stochastic Programming in Dynamic Cognitive Radio Sensor Networks," *IEEE Access*, vol. 9, pp. 720–732, 2020.
- [23] R. Yager, "OWA aggregation over a continuous interval argument with applications to decision making," *IEEE Transactions on Systems, Man, and Cybernetics, Part B (Cybernetics)*, vol. 34, no. 5, pp. 1952–1963, Oct. 2004.
- [24] S. Surekha and M. Z. U. Rahman, "Cognitive Energy-Aware Spectrum Sensing With Improved Throughput for Medical Sensor Networks," *IEEE Sensors Letters*, vol. 6, no. 6, pp. 1–4, Jun. 2022.
- [25] A. Ostovar, Y. B. Zikria, H. S. Kim, and R. Ali, "Optimization of Resource Allocation Model With Energy-Efficient Cooperative Sensing in Green Cognitive Radio Networks," *IEEE Access*, vol. 8, pp. 141 594–141 610, 2020.
- [26] C. Majumdar, D. Lee, A. A. Patel, S. N. Merchant, and U. B. Desai, "Packet Size Optimization for Cognitive Radio Sensor Networks Aided Internet of Things," *IEEE Access*, vol. 5, pp. 6325–6344, 2016.
- [27] Q. Wang, H. Sun, R. Q. Hu, and A. Bhuyan, "When Machine Learning Meets Spectrum Sharing Security: Methodologies and Challenges," *IEEE Open Journal of the Communications Society*, vol. 3, pp. 176–208, 2022.
- [28] Y. Fu and Z. He, "An Online Learning Approach for Cooperator Selection in CSS Under SSDF Attack," *IEEE Communications Letters*, vol. 26, no. 7, pp. 1479–1483, Jul. 2022.
- [29] A. Gao, C. Du, S. X. Ng, and W. Liang, "A Cooperative Spectrum Sensing With Multi-Agent Reinforcement Learning Approach in Cognitive Radio Networks," *IEEE Communications Letters*, vol. 25, no. 8, pp. 2604–2608, Aug. 2021.
- [30] K. L. Ang and J. K. P. Seng, "Application Specific Internet of Things (ASIoTs): Taxonomy, Applications, Use Case and Future Directions," *IEEE Access*, vol. 7, pp. 56 577–56 590, 2019.
- [31] A. E. Abbas and R. A. Howard, *Foundations of Decision Analysis*, 1st ed. Pearson Education Limited, Dec. 2015.
- [32] J. R. Birge and F. Louveaux, *Introduction to Stochastic Programming*, 2nd ed. New York: Springer, Jun. 2011.
- [33] K. Toledo and H. Kaschel, "A Cooperative Spectrum Sensing Strategy for Dynamic Cognitive Radio Sensor Networks," in *2018 IEEE International Conference on Automation/XXIII Congress of the Chilean Association of Automatic Control (ICA-ACCA)*, Concepción, Chile, Oct. 2018, pp. 1–6.
- [34] R. Caballero, E. Cerda, M. M. Muñoz, and L. Rey, "Analysis and comparisons of some solution concepts for stochastic programming problems," *Top*, vol. 10, no. 1, pp. 101–123, Jun. 2002.
- [35] E. Axell and E. G. Larsson, "A Bayesian approach to spectrum sensing, denoising and anomaly detection," in *2009 IEEE International Conference on Acoustics, Speech and Signal Processing*, Apr. 2009, pp. 2333–2336.
- [36] R. R. Yager, "Decision Making Under Dempster–Shafer Uncertainties," in *Classic Works of the Dempster-Shafer Theory of Belief Functions*, ser. Studies in Fuzziness and Soft Computing, R. R. Yager and L. Liu, Eds. Berlin, Heidelberg: Springer, 2008, pp. 619–632.
- [37] R. R. Yager and V. Kreinovich, "Decision making under interval probabilities," *International Journal of Approximate Reasoning*, vol. 22, no. 3, pp. 195–215, Dec. 1999.
- [38] A. Goldsmith, *Wireless Communications*. Cambridge University Press, Aug. 2005.
- [39] S. M. Kay, *Fundamentals of Statistical Signal Processing: Detection Theory*, 1st ed. Englewood Cliffs, N.J.: Prentice Hall, Feb. 1998, vol. II.
- [40] M. Najimi, A. Ebrahimzadeh, and S. M. H. Andargoli, "Energy-efficient cooperative spectrum sensing using two hard decision rules," in *2016 Eighth International Conference on Information and Knowledge Technology (IKT)*, Sep. 2016, pp. 205–210.
- [41] M. A. Matin, *Spectrum Access and Management for Cognitive Radio Networks*, 1st ed., ser. Signals and Communication Technology. Springer Singapore, 2017.
- [42] E. Biglieri, "Spectrum sensing under uncertain channel modeling," *Journal of Communications and Networks*, vol. 14, no. 3, pp. 225–229, Jun. 2012.
- [43] C. Zou, X. Li, X. Liu, and M. Zhang, "3D placement of unmanned aerial vehicles and partially overlapped channel assignment for throughput maximization," *Digital Communications and Networks*, Jul. 2020.
- [44] A. Fotouhi, M. Ding, and M. Hassan, "DroneCells: Improving spectral efficiency using drone-mounted flying base stations," *Journal of Network and Computer Applications*, vol. 174, p. 102895, Jan. 2021.
- [45] T. Instruments, "Low Cost, Low-Power 2.4 GHz RF Transceiver Designed for Low-Power Wireless Apps in the 2.4 GHz ISM B," 2022. [Online]. Available: <https://www.ti.com/product/CC2500?keyMatch=CC2500>
- [46] S. Maleki, A. Pandharipande, and G. Leus, "Energy-Efficient Distributed Spectrum Sensing for Cognitive Sensor Networks," *IEEE Sensors Journal*, vol. 11, no. 3, pp. 565–573, Mar. 2011.
- [47] A. Hatoum, R. Langar, N. Aitsaadi, R. Boutaba, and G. Pujolle, "Cluster-Based Resource Management in OFDMA Femtocell Networks With QoS Guarantees," *IEEE Transactions on Vehicular Technology*, vol. 63, no. 5, pp. 2378–2391, Jun. 2014.
- [48] I. Rhee, M. Shin, S. Hong, K. Lee, S. J. Kim, and S. Chong, "On the Levy-Walk Nature of Human Mobility," *IEEE/ACM Transactions on Networking*, vol. 19, no. 3, pp. 630–643, Jun. 2011.
- [49] J. Harri, F. Filali, and C. Bonnet, "Mobility models for vehicular ad hoc networks: a survey and taxonomy," *IEEE Communications Surveys & Tutorials*, vol. 11, no. 4, pp. 19–41, 2009, conference Name: IEEE Communications Surveys & Tutorials.



**Karel Toledo** received a B.Sc. degree in Telecommunication Engineering and an M.Sc. degree in Digital Systems from the Technological University of Havana, Cuba. Also, he received a Ph.D. degree in Engineering Sciences, mention in Automation from the University of Santiago de Chile, Chile. He is currently an assistant professor at the Department of Electrical Engineering, University of Santiago de Chile, Chile. He has been with the Technological Scientific Center of Valparaíso, Federico Santa María Technical University, as a

postdoctoral researcher and with the Department of Telecommunications and Telematics, Technological University of Havana, CUJAE, Cuba, as a professor. In addition, he has lectured in Digital Signal Processing, Signal Analysis, and Digital Communications. His research interests include wireless communication systems, internet of things, energy efficiency, optimization, and digital signal processing.



**Jorge Torres Gómez** received the B.Sc., M.Sc., and Ph.D. degrees from the Technological University of Havana, CUJAE, Cuba, in 2008, 2010, and 2015, respectively. He is currently with the Telecommunication Networks Group, Department of Telecommunication Systems, Technical University of Berlin. Since 2008, he has been with the School of Telecommunications and Electronics, CUJAE University, where he was a Lecturer from 2008 to 2018. He is a member of the Cuban Association of Pattern Recognition (ACRP). He

has been with the Department of Signal Theory and Communications, Carlos III University of Madrid, Leganés Campus, Madrid, Spain, as a guest lecturer, and with the Department of Digital Signal Processing and Circuit Technology, the Chemnitz University of Technology as a postdoc. His research interests include digital signal processing, software-defined radio, and wireless and wired communication systems.



**Falko Dressler** is full professor and Chair for Data Communications and Networking at the School of Electrical Engineering and Computer Science, TU Berlin. He received his M.Sc. and Ph.D. degrees from the Dept. of Computer Science, University of Erlangen in 1998 and 2003, respectively. Dr. Dressler has been associate editor-in-chief for IEEE Trans. on Mobile Computing and Elsevier Computer Communications as well as an editor for journals such as IEEE/ACM Trans. on Networking, IEEE Trans. on Network Science and

Engineering, Elsevier Ad Hoc Networks, and Elsevier Nano Communication Networks. He has been chairing conferences such as IEEE INFOCOM, ACM MobiSys, ACM MobiHoc, IEEE VNC, IEEE GLOBECOM. He authored the textbooks *Self-Organization in Sensor and Actor Networks* published by Wiley & Sons, and *Vehicular Networking* published by Cambridge University Press. He has been an IEEE Distinguished Lecturer as well

as an ACM Distinguished Speaker. Dr. Dressler is an IEEE Fellow as well as an ACM Distinguished Member. He is a member of the German National Academy of Science and Engineering (acatech). He has been serving on the IEEE COMSOC Conference Council and the ACM SIGMOBILE Executive Committee. His research objectives include adaptive wireless networking (sub-6GHz, mmWave, visible light, molecular communication) and wireless-based sensing with applications in ad hoc and sensor networks, the Internet of Things, and Cyber-Physical Systems.



**M. Julia Fernández-Getino García**, (S'99 - AM'02 - M'03) received the M. Eng. and Ph.D. degrees in telecommunication engineering from the Polytechnic University of Madrid, Spain, in 1996 and 2001, respectively. She is an Associate Professor at the Department of Signal Theory and Communications, Carlos III University of Madrid, Spain. From 1996 to 2001, she held a research position with the Department of Signals, Systems, and Radiocommunications, Polytechnic University of Madrid. She visited Bell Laboratories, Murray

Hill, NJ, USA, in 1998; Lund University, Sweden, during two periods in 1999 and 2000; Politecnico di Torino, Italy, in 2003 and 2004; and Aveiro University, Portugal, in 2009 and 2010. Her research interests include multicarrier communications, coding, and signal processing for wireless systems.

She received the best "Master Thesis" and "Ph.D. Thesis" awards from the Professional Association of Telecommunication Engineers of Spain in 1998 and 2003, respectively; the "Student Paper Award" at the IEEE International Symposium on Personal, Indoor and Mobile Radio Communications (PIMRC) in 1999; the "Certificate of Appreciation" at the IEEE Vehicular Technology Conference (VTC) in 2000; the "Ph.D. Extraordinary Award" from the Polytechnic University of Madrid in 2004; the "Juan de la Cierva National Award" from AENA Foundation in 2004; and the "Excellence Award" from Carlos III University of Madrid in 2012 to her research career.